ISIT'2013 1569719559

Scalar Quantize-and-Forward for Symmetric Half-duplex Two-Way Relay Channels

Michael Heindlmaier, Onurcan İşcan
Institute for Communications Engineering
Technische Universität München, Munich, Germany
Email: michael.heindlmaier@tum.de, onurcan.iscan@tum.de

Christopher Rosanka
Rohde & Schwarz
Munich, Germany
Email: ch.rosanka@mytum.de

***Abstract*—Scalar Quantize & Forward (QF) schemes are studied for the Two-Way Relay Channel. Different QF approaches are compared in terms of rates as well as relay and decoder complexity. A coding scheme not requiring Slepian-Wolf coding at the relay is proposed and properties of the corresponding sum-rate optimization problem are presented. An iterative numerical scheme is derived that guides optimized quantizer design. The results are supported by simulations.**

I. Introduction

Consider a communication system where two nodes T_1 and T_2 wish to communicate to each other with the help of a relay r and there is no direct link between T_1 and T_2. This scenario is known as a separated two-way relay channel (TWRC) [1], [2] and it incorporates challenging problems such as multiple access, broadcast, and coding with side information.

In this work, we focus on Quantize & Forward (QF) relaying: The relay maps its received (noisy) signal to a quantization index by using a quantizer function $\mathcal{Q}(.)$. The index is then digitally transmitted to the destination nodes through the downlink channels. We use information theoretic arguments to find quantizers that almost maximize the sum-rate, an approach that has been proposed in [3] and [4] in a similar context.

In general, *vector* quantizers give the best performance, but under certain conditions *scalar* quantizers almost maximize the sum-rate. Scalar quantizers are attractive because of their design and implementation simplicity.

Our main focus is the symmetric TWRC, where both users' channel qualities are the same, both in the uplink and downlink. We describe the system model in Sec. II, and in Sec. III we compare different achievable rate regions for the TWRC. We introduce a new rate region that is smaller than previous regions, but almost as large for the symmetric TWRC. The achievability scheme does not require the relay to employ Slepian-Wolf Coding. In Sec. IV, we look at the sum-rate optimization and quantizer design problems and propose a numerical solution. Examples of optimal quantizers are given and optimal time sharing parameters are calculated. In Sec. V we evaluate the performance of the optimized system by simulations. Sec. VI concludes our work.

II. System Model

The system has two source nodes T_1 and T_2 that exchange their independent messages $W_1 \in \{1, 2, \ldots, 2^{nR_1}\}$, $W_2 \in \{1, 2, \ldots, 2^{nR_2}\}$ in n channel uses through a relay node r. The source nodes cannot hear each other, so communication is possible only through the relay. The communication is split into two phases: In the multiple access (MAC) phase with n_{MAC} channel uses, both source nodes encode their messages W_1 and W_2 to the MAC channel inputs $X_1^{n_{\text{MAC}}}$ and $X_2^{n_{\text{MAC}}}$, respectively, with $X_{1,t} \in \mathcal{X}_1$, $X_{2,t} \in \mathcal{X}_2$. Define $\alpha = n_{\text{MAC}}/n$ as the time fraction of this first phase. The relay receives

$$Y_{r,t} = X_{1,t} + X_{2,t} + Z_{r,t}, \quad t = \{1, 2, \ldots, n_{\text{MAC}}\}, \qquad (1)$$

where $Z_{r,t} \sim \mathcal{N}(0, N_r)$ and $\mathbb{E}\{X_{1,t}^2\} \leq P_1$, $\mathbb{E}\{X_{2,t}^2\} \leq P_2$.

The relay maps $Y_r^{n_{\text{MAC}}}$ to a quantized representation $\hat{Y}_r^{n_{\text{MAC}}}$ with symbol alphabet $\hat{\mathcal{Y}}_r$. The associated quantizer index is $q = \mathcal{Q}(Y_r^{n_{\text{MAC}}})$. During the Broadcast (BC) phase with $n_{\text{BC}} = n - n_{\text{MAC}}$ channel uses, the relay transmits the codeword $X_r^{n_{\text{BC}}}(q)$. The received signals at T_1 and T_2 are:

$$Y_{j,t} = X_{r,t} + Z_{j,t}, \quad t = \{n_{\text{MAC}} + 1, \ldots, n\}, \qquad (2)$$

for $j \in \{1, 2\}$, $\mathbb{E}\{X_{r,t}^2\} \leq P_r$ and $Z_{j,t} \sim \mathcal{N}(0, N_j)$. Nodes T_1 and T_2 decode W_2 and W_1, respectively, by using their own message as side information. Fig. 1 depicts the system setup. In the following, we often omit the time index t if we refer to a single channel use. We focus on one-dimensional modulation schemes to reduce computational complexity for simulations. All results apply to complex signaling as well.

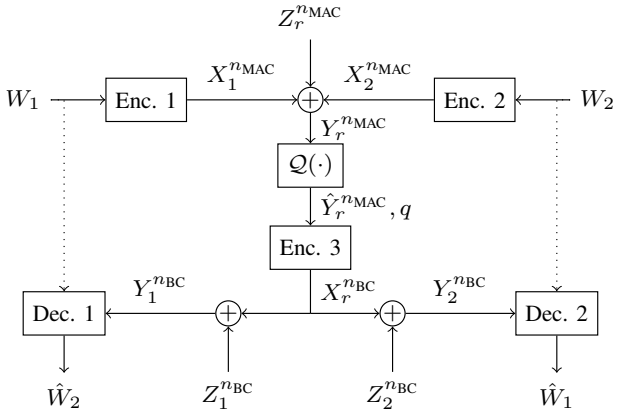

Fig. 1: System block diagram.

In the next section we review different coding schemes and compare their performance.

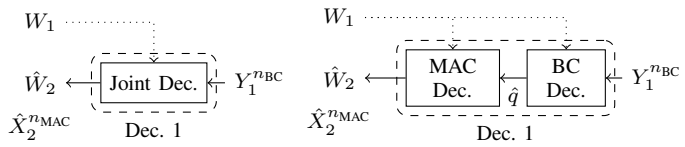

(a) Decoder for $\mathcal{R}_{\text{NNC}}$. (b) Decoder for $\mathcal{R}_{\text{CF}}$.

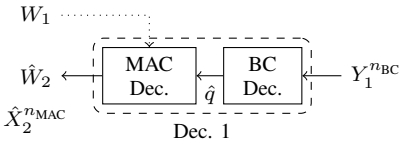

(c) Decoder for $\mathcal{R}_{\text{NoSW}}$.

Fig. 2: Decoder structure for different schemes.

III. Achievable Rates

A. Noisy Network Coding / Joint Decoding

In [5], an achievable rate region was derived that matches the rates achieved with Noisy Network Coding (NNC) [6]. The closure of the achievable rate region is given by the set $\mathcal{R}_{\text{NNC}} \subset \mathbb{R}_+^2$ of rate tuples (R_1, R_2) satisfying

$$\begin{aligned} R_1 &\le \alpha I(X_1; \hat{Y}_r | X_2, U) \\ R_1 &\le (1-\alpha) I(X_r; Y_2) - \alpha I(Y_r; \hat{Y}_r | X_1, X_2, U) \\ R_2 &\le \alpha I(X_2; \hat{Y}_r | X_1, U) \\ R_2 &\le (1-\alpha) I(X_r; Y_1) - \alpha I(Y_r; \hat{Y}_r | X_1, X_2, U) \end{aligned} \tag{3}$$

for some $p(u)p(x_1|u)p(x_2|u)p(y_r|x_1,x_2)p(\hat{y}_r|y_r)$ and $p(x_r)p(y_1,y_2|x_r)$ and $\alpha > 0$. It suffices to consider $|\hat{\mathcal{Y}}_r| \le |\mathcal{Y}_r| + 2$, $|\mathcal{U}| \le 3$.

1) Receivers: To achieve a rate tuple in $\mathcal{R}_{\text{NNC}}$, the decoder must jointly decode the BC code and the MAC code in a single stage decoder using its own message as side information. The quantization index q is not required to be decoded. The decoder structure is shown in Fig. 2a.

2) Gaussian Case: For the Gaussian case, $X_1 \sim \mathcal{N}(0, P_1)$, $X_2 \sim \mathcal{N}(0, P_2)$, $X_r \sim \mathcal{N}(0, P_r)$ and $Y_r \sim \mathcal{N}(0, P_1 + P_2 + N_r)$. We choose a (not necessarily optimal) quantizer yielding $\hat{Y}_r = Y_r + \hat{Z}$, where the quantization noise $\hat{Z} \sim \mathcal{N}(0, \hat{N})$ is independent of Y_r. Define $C(x) := \frac{1}{2}\log(1+x)$. With $\mathcal{U} = \emptyset$, the achievable rate region becomes

$$\begin{aligned} R_1 &\le \min\left\{ \alpha C\left(\frac{P_1}{N_r + \hat{N}}\right), (1-\alpha) C\left(\frac{P_r}{N_2}\right) - \alpha C\left(\frac{N_r}{\hat{N}}\right) \right\} \\ R_2 &\le \min\left\{ \alpha C\left(\frac{P_2}{N_r + \hat{N}}\right), (1-\alpha) C\left(\frac{P_r}{N_1}\right) - \alpha C\left(\frac{N_r}{\hat{N}}\right) \right\}. \end{aligned} \tag{4}$$

B. Compress & Forward

In the spirit of classic Compress & Forward (CF), the authors of [7], [8] derive an achievable rate region generalizing [2] using ideas from [9]. The achievable rate region is the set $\mathcal{R}_{\text{CF}} \subset \mathbb{R}_+^2$ of rate tuples (R_1, R_2) satisfying

$$\begin{aligned} R_1 \le \alpha I(X_1; \hat{Y}_r | X_2, U), \quad R_2 \le \alpha I(X_2; \hat{Y}_r | X_1, U) \\ \text{for} \quad \alpha I(Y_r; \hat{Y}_r | X_2, U) \le (1-\alpha) I(X_r; Y_2) \\ \alpha I(Y_r; \hat{Y}_r | X_1, U) \le (1-\alpha) I(X_r; Y_1) \end{aligned} \tag{5}$$

for some $p(u)p(x_1|u)p(x_2|u)p(y_r|x_1,x_2)p(\hat{y}_r|y_r)$ and $p(x_r)p(y_1,y_2|x_r)$, $\alpha > 0$. It suffices to consider $|\hat{\mathcal{Y}}_r| \le |\mathcal{Y}_r| + 3$, $|\mathcal{U}| \le 4$.

1) Receivers: The coding scheme of [7] requires reliable decoding of the quantization index q at the receiver. For that, the BC code is decoded using the own message as a priori knowledge. Knowing q, the desired message is decoded, again using the own message as side information. The structure of this decoder is shown in Fig. 2b.

2) Gaussian Case: With the same assumptions as before, i.e. $\hat{Y}_r = Y_r + \hat{Z}$, one obtains:

$$\begin{aligned} R_1 \le \alpha C\left(\frac{P_1}{N_r + \hat{N}}\right), \quad R_2 \le \alpha C\left(\frac{P_2}{N_r + \hat{N}}\right) \\ \text{for} \quad \alpha C\left(\frac{P_1 + N_r}{\hat{N}}\right) \le (1-\alpha) C\left(\frac{P_r}{N_2}\right) \\ \alpha C\left(\frac{P_2 + N_r}{\hat{N}}\right) \le (1-\alpha) C\left(\frac{P_r}{N_1}\right). \end{aligned} \tag{6}$$

C. Neglecting Side Information in the Downlink

The coding scheme for CF requires Slepian-Wolf (SW) coding [10] at the relay to reduce the downlink rate. In the symmetric case we do not expect this reduction to be substantial. We are thus interested in schemes without SW coding in the BC phase. Using random coding arguments, the achievable rates are given by the set $\mathcal{R}_{\text{NoSW}} \subset \mathbb{R}_+^2$ of rate tuples (R_1, R_2) satisfying

$$\begin{aligned} R_1 \le \alpha I(X_1; \hat{Y}_r | X_2, U), \quad R_2 \le \alpha I(X_2; \hat{Y}_r | X_1, U) \\ \text{for } \alpha I(Y_r; \hat{Y}_r | U) \le (1-\alpha) \min\{ I(X_r; Y_2), I(X_r; Y_1) \} \end{aligned} \tag{7}$$

for some $p(u)p(x_1|u)p(x_2|u)p(y_r|x_1,x_2)p(\hat{y}_r|y_r)$ and $p(x_r)p(y_1,y_2|x_r)$, $\alpha > 0$. Similarly, we have $|\mathcal{U}| \le 4$ and $|\hat{\mathcal{Y}}_r| \le |\mathcal{Y}_r| + 3$. A proof of this claim can be found in [11].

1) Receivers: The structure of the decoder is shown in Fig. 2c. Similar to the scheme in Sect. III-B, two decoding stages are required: First the BC code is decoded, revealing q reliably. Then q is used to obtain the desired message from the MAC code. In contrast to before, the own message is used only in the MAC decoder.

2) Gaussian Case: The rate region is described by

$$\begin{aligned} R_1 \le \alpha C\left(\frac{P_1}{N_r + \hat{N}}\right), \quad R_2 \le \alpha C\left(\frac{P_2}{N_r + \hat{N}}\right) \\ \alpha C\left(\frac{P_1 + P_2 + N_r}{\hat{N}}\right) \le (1-\alpha) \min\left\{ C\left(\frac{P_r}{N_2}\right), C\left(\frac{P_r}{N_1}\right) \right\} \end{aligned}$$

D. Sum-Rate Comparison for Gaussian Case

Note that in general $\mathcal{R}_{\text{NoSW}} \subset \mathcal{R}_{\text{CF}} \subset \mathcal{R}_{\text{NNC}}$. We focus on the maximal sum rate $R_1 + R_2$ for each scheme in the symmetric Gaussian case $P_1 = P_2 = P$, $N_1 = N_2 = N$.

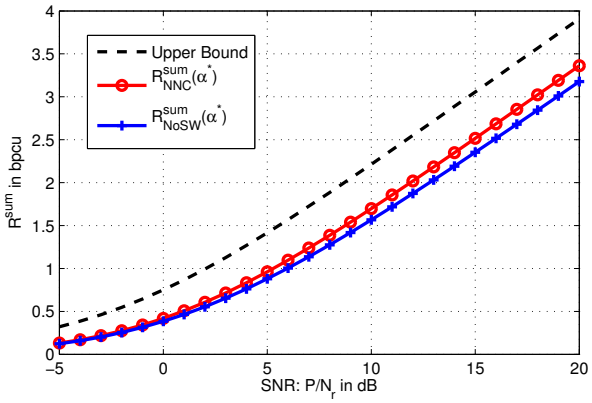

Fig. 3: Sum rates $R^{\text{sum}}_{\text{CF}}(\alpha^*) = R^{\text{sum}}_{\text{NNC}}(\alpha^*)$ and $R^{\text{sum}}_{\text{NoSW}}(\alpha^*)$ as a function of SNR:= P/N_r and $P_r = P + 8.5$dB. The upper bound is $\min\{2\alpha\mathcal{C}(P/N_r), 2(1-\alpha)\mathcal{C}(P_r/N)\}$.

This requires to jointly optimize over the quantization noise variance $\hat{N}$ and time allocation α. Formally, define

$$R^{\text{sum}}_{\text{NNC}}(\alpha) := \max_{\hat{N}}(R_1 + R_2), \quad (R_1, R_2) \in \mathcal{R}_{\text{NNC}}$$

and similarly for $R^{\text{sum}}_{\text{CF}}(\alpha)$ and $R^{\text{sum}}_{\text{NoSW}}(\alpha)$. The optimal sum rate is

$$R^{\text{sum}}(\alpha) = 2\alpha\mathcal{C}\left(\frac{P}{N_r + \hat{N}^*(\alpha)}\right) \tag{8}$$

for all three schemes. The only difference is the optimal value of $\hat{N}$ for a given α, denoted by $\hat{N}^*(\alpha)$. For $\mathcal{R}_{\text{NoSW}}$, we have

$$\hat{N}^*_{\text{NoSW}}(\alpha) = \frac{2P + N_r}{(1 + P_r/N)^{(1-\alpha)/\alpha} - 1}$$

because the sum rate is decreasing in $\hat{N}$ and $\hat{N}^*_{\text{NoSW}}(\alpha)$ is the smallest variance satisfying the constraints. Similarly, for $\mathcal{R}_{\text{CF}}$, we have

$$\hat{N}^*_{\text{CF}}(\alpha) = \frac{P + N_r}{(1 + P_r/N)^{(1-\alpha)/\alpha} - 1}.$$

As $\hat{N}^*_{\text{CF}}(\alpha) < \hat{N}^*_{\text{NoSW}}(\alpha)$, we have $R^{\text{sum}}_{\text{CF}}(\alpha) > R^{\text{sum}}_{\text{NoSW}}(\alpha)$. For $\mathcal{R}_{\text{NNC}}$, the rate expressions for NNC in Eq. (4) are either increasing or decreasing in $\hat{N}$. The maximum with respect to $\hat{N}$ is thus found at the crossing point of both expressions. It is not hard to show that $\hat{N}^*_{\text{NNC}}(\alpha) = \hat{N}^*_{\text{CF}}(\alpha)$ (see [11] for a derivation). This means, given the assumption that $(Y_r, \hat{Y}_r)$ are jointly Gaussian, NNC does not provide higher sum rates than CF in the symmetric case.

Fig. 3 shows achievable sum rates over SNR for the symmetric Gaussian case. For each curve, the value of α was chosen to maximize the sum rate. The difference between $R^{\text{sum}}_{\text{CF}}(\alpha^*) = R^{\text{sum}}_{\text{NNC}}(\alpha^*)$ and $R^{\text{sum}}_{\text{NoSW}}(\alpha^*)$ is small here. We expect that this trend holds also for other input distributions.

The scheme corresponding to $R^{\text{sum}}_{\text{NoSW}}(\alpha^*)$ requires less complex relay operations. This motivates us to focus on this scheme, accepting a slightly smaller achievable sum rate. Also note that we assume that $\mathcal{U} = \emptyset$.

IV. Quantizer Design

A. Sum-Rate Optimization for $\mathcal{R}_{NoSW}$

To guide the quantizer design for DMCs and fixed discrete input distributions, we want to find the optimal conditional probability mass function (pmf) $p(\hat{y}_r|y_r)$ and time sharing coefficient α to optimize the sum-rate. With $C := \min\{I(X_r;Y_2), I(X_r;Y_1)\}$ as the downlink capacity, this problem can be stated as

$$\begin{aligned} R^{\text{sum}}_{\text{NoSW}} := \sup_{\alpha, p(\hat{y}_r|y_r)} \; & \alpha\Big(I(X_1;\hat{Y}_r|X_2) + I(X_2;\hat{Y}_r|X_1)\Big) \\ \text{subject to:} \quad & \alpha I(Y_r;\hat{Y}_r) \le (1-\alpha)C. \end{aligned} \tag{9}$$

Abbreviate $p(\hat{y}_r|y_r)$ by p and let $p_{ij} := p(\hat{y}_{ri}|y_{rj})$: Denote the objective as $J(p) := I(X_1;\hat{Y}_r|X_2) + I(X_2;\hat{Y}_r|X_1)$ and define the function

$$I(C) := \sup_{p(\hat{y}_r|y_r): I(Y_r;\hat{Y}_r) \le C} J(p). \tag{10}$$

Problem (9) can be stated as

$$R^{\text{sum}}_{\text{NoSW}} = \max_{\alpha} \alpha I\left(\frac{1-\alpha}{\alpha}C\right). \tag{11}$$

Some properties of $I(C)$ are as follows:

1) The functions $I(X_1;\hat{Y}_r|X_2) + I(X_2;\hat{Y}_r|X_1)$ and $I(Y_r;\hat{Y}_r)$ are convex in $p(\hat{y}_r|y_r)$ [12, Theorem 2.7.4]. Program (10) is thus a convex maximization, a difficult problem in general. From the *maximum principle* [13, Cor. 32.3.2], it follows that for the optimal $p(\hat{y}_r|y_r)$, $I(Y_r;\hat{Y}_r) = C$, for $0 \le C \le H(Y_r)$.
2) $I(C)$ is an increasing and concave function in C, for $0 \le C \le H(Y_r)$, and it is sufficient to choose $|\hat{\mathcal{Y}}_r| \le |\mathcal{Y}_r| + 1$. The proof is along the lines of [14]. We refer to [11] for a more detailed derivation.

Fig. 4 shows one example of $I(C)$. $L = |\hat{\mathcal{Y}}_r|$ represents the number of different quantization levels. One can observe that it suffices to consider only a relatively small L. For example, using a mapping with $L = 8$ quantization levels instead of $L = 16$ causes a rate reduction of less then 0.03 in $I(C)$.

B. Computing the Function $I(C)$

To solve the problem for $I(C)$ in Eq. (10), similar to [12, Section 10] we write the Lagrangian:

$$\mathcal{L}(p, \lambda, \nu_1, \ldots, \nu_L) = J(p) - \lambda I(Y_r;\hat{Y}_r) + \sum_j \nu_j \sum_i p_{ij},$$

$\lambda \ge 0$, where the last constraints force $p(\hat{y}_r|y_r)$ to be a valid pmf. The KKT conditions require

$$\frac{\partial \mathcal{L}}{\partial p_{ij}} = \frac{\partial J}{\partial p_{ij}} - \lambda p(y_{rj}) \log \frac{p_{ij}}{p(\hat{y}_{ri})} + \nu_j \stackrel{!}{=} 0, \quad \forall\, i, j. \tag{12}$$

With the substitution

$$\log \mu_j := -\frac{\nu_j}{\lambda p(y_{rj})} \quad \Leftrightarrow \quad \nu_j = -\lambda p(y_{rj}) \log \mu_j$$

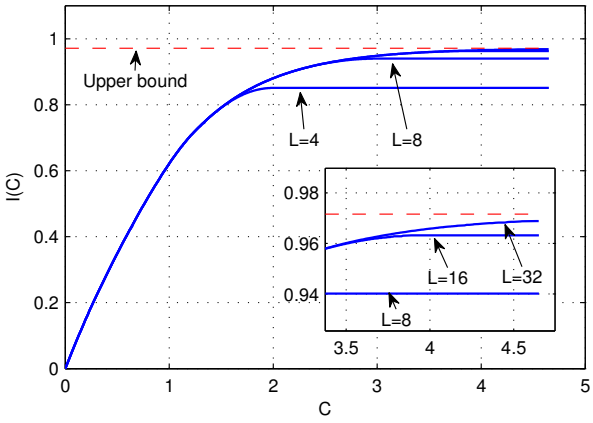

Fig. 4: $I(C)$ and upper bound $I(X_1;Y_r|X_2)+I(X_2;Y_r|X_1)$ for BPSK modulation at both users and $P=0$dB, $N=0$dB, for different numbers of quantization levels $L=|\hat{\mathcal{Y}}_r|$.

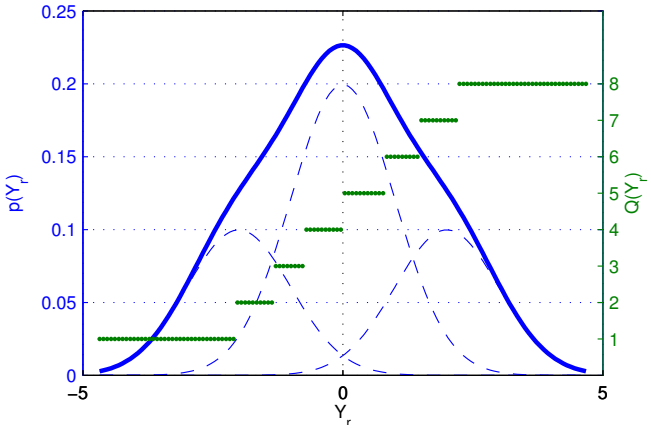

Fig. 5: Numerically optimized quantizer function (dotted line) and $p(y_\mathrm{r})$ (solid line). Note that the solid curve represents the sum of the dashed curves which correspond to the pdfs conditioned on X_1+X_2.

it follows that $p_{ij} = \frac{p(\hat{y}_{ri})}{\mu_j}\exp\left(\frac{\frac{\partial J}{\partial p_{ij}}}{\lambda p(y_{rj})}\right)$. But since $\sum_k p_{kj} \stackrel{!}{=} 1$ for all j, we obtain $\mu_j = \sum_k p(\hat{y}_{rk})\exp\left(\frac{\frac{\partial J}{\partial p_{kj}}}{\lambda p(y_{rj})}\right), \forall\ j$.
The optimality conditions are thus given by

$$p_{ij} = p(\hat{y}_{ri}|y_{rj}) = \frac{p(\hat{y}_{ri})\exp\left(\frac{\frac{\partial J}{\partial p_{ij}}}{\lambda p(y_{rj})}\right)}{\sum_k p(\hat{y}_{rk})\exp\left(\frac{\frac{\partial J}{\partial p_{kj}}}{\lambda p(y_{rj})}\right)}, \quad \forall\ i,j, \quad (13)$$

$$p(\hat{y}_{ri}) = \sum_j p(\hat{y}_{ri}|y_{rj})p(y_{rj}), \quad \forall\ i. \quad (14)$$

One can solve for a conditional pmf $p(\hat{y}_r|y_r)$ satisfying Eqs. (13, 14) with a fixed-point-iteration with an initial value for p, similar to the Blahut-Arimoto algorithm (e.g. [12, Section 10.8]). Different initial values for p can result in different outcomes. In practice, we start the iteration with different initial values and store the best result.

C. Scalar vs. Vector Quantization

In general, a vector quantizer must be used at the relay to achieve the rate regions in Sec. III. An ideal vector quantizer results in a pmf $p(\hat{y}_r|y_r)$ that optimizes the problem in Eq. (10). A scalar quantizer permits only deterministic single-letter relationships, i.e. we have

$$p(\hat{y}_{ri_j}|y_{rj}) = 1 \text{ for one particular } i_j,\ \forall\ j. \quad (15)$$

If (15) is fulfilled for the optimal pmf, the quantizer function $\mathcal{Q}(.)$ can be directly inferred. In the saturation region in the curves in Fig. 4 one obtains scalar quantizers since $C > \log(L) \geq I(Y_r;\hat{Y}_r)$. In this case the constraints for problem (10) are only those for a valid pmf. As a convex maximization is optimized at one of its corner points [13, Cor. 32.3.2], (15) will be fulfilled. We see that the loss by using a scalar quantizer is small for sufficiently large L and proceed with this more practical method.

D. Optimized Time Allocation

$I(C)$ in Eq. (10) captures the optimization of the pmf $p(\hat{y}_r|y_r)$ in problem (9). To optimize also the time allocation parameter α, we must solve the problem in Eq. (11).

Proposition 1: The function $\alpha I\left(\frac{1-\alpha}{\alpha}C\right)$ is concave in α, where C is a positive constant independent of α.

Proof: From property 2) in Sec. IV-A we known that $I'(C) := \frac{\partial I(C)}{\partial C} = \lambda \geq 0$ and $I''(C) := \frac{\partial^2 I(C)}{\partial C^2} \leq 0$. Define the function $h(\alpha) := \frac{1-\alpha}{\alpha}C$ for $0<\alpha\leq 1$. Note that

$$h'(\alpha) := \frac{\partial h(\alpha)}{\partial \alpha} = -\frac{1}{\alpha^2}C < 0 \text{ and}$$
$$h''(\alpha) := \frac{\partial^2 h(\alpha)}{\partial \alpha^2} = \frac{2}{\alpha^3}C > 0.$$

Further note that $h'(\alpha) = -\frac{\alpha}{2}h''(\alpha)$ and

$$\frac{\partial^2\left(\alpha I(h(\alpha))\right)}{\partial \alpha^2} = 2I'(h(\alpha))\cdot h'(\alpha) + \alpha I'(h(\alpha))\cdot h''(\alpha) + \alpha I''(h(\alpha))\cdot h'(\alpha)^2. \quad (16)$$

As $h'(\alpha) = -\frac{\alpha}{2}h''(\alpha)$, the first two summands add to zero and only the last summand remains. This term is always at most 0, proving that $\frac{\partial^2(\alpha I(h(\alpha)))}{\partial \alpha^2} \leq 0$ for $0<\alpha\leq 1$. ■
Prop. 1 shows that there is a unique maximizer α for the optimal sum-rate that can be found efficiently once $I(C)$ or an approximation of it is known.

V. Performance Evaluation

Using the method of the previous section, we obtain a mapping for the following parameters: $P=0$dB, $P_r=9.3$dB, $N_r=N=0$dB, $L=8$, $\alpha=1/3$. The resulting quantizer fulfills the criteria in (15) (and is thus a scalar quantizer) and gives the sum-rate 0.29. This mapping is shown in Fig. 5 together with $p(y_\mathrm{r})$.

We evaluate the performance of this mapping by means of numerical simulations. As channel codes, we use the

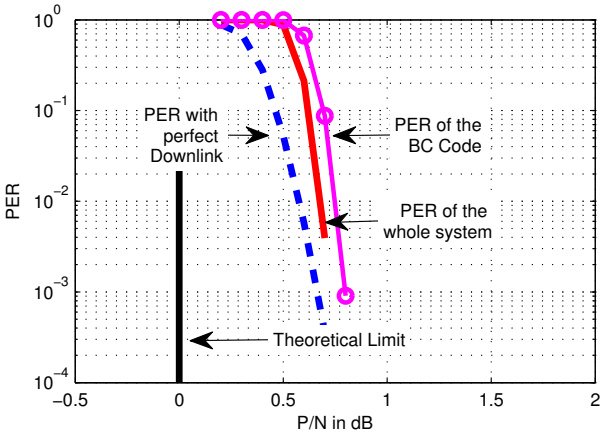

Fig. 6: Packet Error Rate (PER) simulations for the system with the quantizer given in Fig. 5.

IRA-LDPC codes of the DVB-S2 standard [15]. In the uplink, blocks of $k_1 = k_2 = 7200$ information bits are encoded with the rate 0.444 (MAC Code) to blocks of $n_{\text{MAC}} = 16200$ BPSK symbols that are transmitted from T_1 and T_2 to r during the MAC phase. The received 16200 samples at r are mapped according to the quantizer to 16200 symbols, that are represented by $16200 \cdot \log(L) = 48600$ bits[1]. These bits are encoded by a channel code (BC Code) of rate $3/4$ to 64800 downlink code bits that are broadcast to T_1 and T_2 during the BC phase with $n_{\text{BC}} = 32400$ 4-PAM symbols. As a result, for the transmission of one block $n_{\text{MAC}} = 16200$ symbols are used in the uplink and $n_{\text{BC}} = 32400$ symbols are used in the downlink, which corresponds to $\alpha = 1/3$. The sum-rate of the system ($(k_1 + k_2)/(n_{\text{MAC}} + n_{\text{BC}}) = 0.29$ bits/channel use), the time sharing parameter and the transmit powers of the nodes match the optimization parameters of the quantizer. At the receivers, we use the approach given in Sec. III-C for decoding: first, the relay quantization index $\hat{q}$ is decoded without using side information. By using $\hat{q}$ and transmitted own symbol, the LLR of the other user's symbol is calculated which is fed to the MAC decoder.

During the simulation, the noise level is varied and the packet error rates are evaluated accordingly. Fig. 6 depicts the PER vs. uplink SNR. Recall that the noise powers used in the optimization for this example are chosen as 0dB, which corresponds to an uplink SNR of 0dB. Therefore the PER is expected to approach zero at 0 dB. The gap to this theoretical limit is about 0.75dB. As the DVB-S2 LDPC codes are about 0.7-1.2dB away from the Shannon limit in point-to-point channels [15] the simulations verify our quantizer design. Fig. 6 also shows the PER performance of the BC code (curve with circle marker) and the PER of the system with perfect downlink channels (dashed line). These curves give insight: The gap between the dashed line and the solid line can be seen as the loss due to the imperfect BC code and the gap between the theoretical limit and the dashed line can be interpreted as the loss due to the imperfect MAC code and the quantizer loss. Moreover, it is interesting that the PER of the complete system is less than the PER of BC code. This is because even if some of the quantization indices are transmitted erroneously during the BC phase, they are corrected by the MAC code.

[1]In general, $\hat{Y}_r$ is not uniformly distributed and hence source coding should be performed before transmitting the indices. However, in this specific example $H(\hat{Y}_r) \approx 3$ and therefore source coding can be omitted.

VI. Conclusion

We compared different QF schemes for the separated TWRC. We showed that the loss caused by neglecting Slepian-Wolf coding in the broadcast code can be small for symmetric setups, but it allows less complex operations at the relay and decoder. A numerical method to maximize the sum-rate and guide quantizer design was derived and applied to special parameters. We observed that the loss due to scalar instead of vector quantization is small. Simulations support our results and show that practical schemes are close to the predicted limits. The study of asymmetric scenarios is left as future work.

Acknowledgments

The authors are supported by the German Ministry of Education and Research in the framework of the Alexander von Humboldt-Professorship and by the grant DLR@Uni of the Helmholtz Allianz. The authors thank Prof. Gerhard Kramer for his helpful comments.

References

[1] D. Gunduz, E. Tuncel, and J. Nayak, "Rate regions for the separated two-way relay channel," in *Allerton Conf. Communication, Control and Computing*, Monticello, IL, Sep. 2008, pp. 1333–1340.

[2] B. Rankov and A. Wittneben, "Achievable rate regions for the two-way relay channel," in *IEEE Int. Symp. Inf. Theory*, Seattle, Jul. 2006, pp. 1668–1672.

[3] A. Winkelbauer and G. Matz, "Soft-information-based joint network-channel coding for the two-way relay channel," in *Int. Symp. Network Coding*, Beijing, Jul. 2011, pp. 1–5.

[4] G. Zeitler, "Low-precision quantizer design for communication problems," Ph.D. dissertation, Technische Universität München, 2012.

[5] C. Schnurr, S. Stanczak, and T. Oechtering, "Coding theorems for the restricted half-duplex two-way relay channel with joint decoding," in *IEEE Int. Symp. Inf. Theory*, Toronto, Jul. 2008, pp. 2688–2692.

[6] S. Lim, Y. Kim, A. El Gamal, and S. Chung, "Noisy network coding," *IEEE Trans. Inf. Theory*, vol. 57, no. 5, pp. 3132–3152, 2011.

[7] C. Schnurr, T. Oechtering, and S. Stanczak, "Achievable rates for the restricted half-duplex two-way relay channel," in *Asilomar Conf. Signals, Systems and Computers*, Pacific Grove, CA, Nov. 2007, pp. 1468–1472.

[8] S. J. Kim, N. Devroye, P. Mitran, and V. Tarokh, "Achievable rate regions and performance comparison of half duplex bi-directional relaying protocols," *IEEE Trans. Inf. Theory*, vol. 57, no. 10, pp. 6405 –6418, Oct. 2011.

[9] E. Tuncel, "Slepian-wolf coding over broadcast channels," *IEEE Trans. Inf. Theory*, vol. 52, no. 4, pp. 1469–1482, 2006.

[10] D. Slepian and J. Wolf, "Noiseless coding of correlated information sources," *IEEE Trans. Inf. Theory*, vol. 19, no. 4, pp. 471–480, 1973.

[11] M. Heindlmaier, O. İşcan, and C. Rosanka, "Scalar quantize-and-forward for symmetric half-duplex two-way relay channels (extended version)," 2013. [Online]. Available: http://de.arxiv.org/abs/1301.6397

[12] T. Cover and J. Thomas, *Elements of information theory*. Wiley, 2006.

[13] R. Rockafellar, *Convex analysis*. Princeton University Press, 1997.

[14] H. Witsenhausen and A. Wyner, "A conditional entropy bound for a pair of discrete random variables," *IEEE Trans. Inf. Theory*, vol. 21, no. 5, pp. 493–501, 1975.

[15] A. Morello and V. Mignone, "DVB-S2: The Second Generation Standard for Satellite Broad-Band Services," *Proc. IEEE*, vol. 94, no. 1, pp. 210–227, 2006.